Derivation of climate elasticity of runoff to assess the effects of climate change on annual runoff

Hanbo Yang[1] and Dawen Yang[1]

Received 10 March 2010; revised 1 May 2011; accepted 9 May 2011; published 14 July 2011.

[1] Climate elasticity of runoff is an important indicator for evaluating the effects of climate change on runoff. Consequently, this paper proposes an analytical derivation of climate elasticity. Based on the mean annual water-energy balance equation, two dimensionless numbers (the elasticities of runoff to precipitation and potential evaporation) were derived. Combining the first-order differential of the Penman equation, the elasticities of runoff to precipitation, net radiation, air temperature, wind speed, and relative humidity were derived to separate the contributions of different climatic variables. The case study was carried out in the Futuo River catchment in the Hai River basin, as well as in 89 catchments of the Hai River and the Yellow River basins of China. Based on the mean annual of climatic variables, the climate elasticity in the Futuo River basin was estimated as follows: precipitation elasticity $\varepsilon_P = 2.4$, net radiation elasticity $\varepsilon_{\mathrm{Rn}} = -0.8$, air temperature elasticity $\varepsilon_T = -0.05°\mathrm{C}^{-1}$, wind speed elasticity $\varepsilon_U = -0.3$, and relative humidity elasticity $\varepsilon_{\mathrm{RH}} = 0.8$. In this catchment, precipitation decrease was mainly responsible for runoff decline, and wind speed decline had the second greatest effect on runoff. In the 89 catchments of the Hai River and the Yellow River basins of China, climate elasticity was estimated as follows: ε_P ranging from 1.6 to 3.9, $\varepsilon_{\mathrm{Rn}}$ ranging from -1.9 to -0.3, ε_T ranging from -0.11 to $-0.02°\mathrm{C}^{-1}$, ε_U ranging from -0.8 to -0.1, and $\varepsilon_{\mathrm{RH}}$ ranging from 0.2 to 1.9. Additional analysis shows that climate elasticity was sensitive to catchment characteristics.

Citation: Yang, H., and D. Yang (2011), Derivation of climate elasticity of runoff to assess the effects of climate change on annual runoff, *Water Resour. Res., 47*, W07526, doi:10.1029/2010WR009287.

1. Introduction

[2] In recent years, climate change has become increasingly significant [*IPCC*, 2007]. Hence, assessing the impacts of climate change on the hydrologic cycle is an important issue for the development of hydrology and water resource management. On a catchment scale, climate elasticity of runoff is considered an important indicator quantifying the sensitivity of runoff to climate change [e.g., *Dooge et al.*, 1999; *Dooge*, 1992; *Fu et al.*, 2007; *Milly and Dunne*, 2002; *Sankarasubramanian et al.*, 2001; *Schaake*, 1990; *Zheng et al.*, 2009]. Climate elasticity of runoff can be defined as the proportional change in runoff (R) to the change in climatic variables [*Fu et al.*, 2007]. Precipitation (P) has an important impact on runoff. The relationship of elasticity of runoff (R) to P was first defined by *Schaake* [1990] as

$$\varepsilon_P(P,R) = \frac{dR}{dP}\frac{P}{R}\ . \quad (1)$$

Ignoring the impacts of other factors on runoff, equation (1) can be transformed into

$$\frac{dR}{R} = \varepsilon_P(P,R)\frac{dP}{P}\ . \quad (2)$$

[1]State Key Laboratory of Hydro-Science and Engineering, Department of Hydraulic Engineering, Tsinghua University, Beijing, China.

0043-1397/11/2010WR009287

[3] Based on equation (2), several studies have investigated the response of annual runoff to precipitation change [e.g., *Chiew*, 2006; *Niemann and Eltahir*, 2005; *Sankarasubramanian and Vogel*, 2003]. Climate elasticity, which quantifies the hydrologic response to climate change, implies a method for assessing runoff change in the future. Based on the precipitation elasticity of runoff of 2–3 in Southeast Australia, -10 to $+3$% changes in the future mean annual precipitation are projected to lead to -23 to $+4$% changes in the mean annual runoff [*Chiew et al.*, 2009]. *Gardner* [2009] estimated climate elasticity of annual runoff and then evaluated runoff changes in North America using the A1B Emissions Scenario that was presented by the Intergovernmental Panel on Climate Change [*IPCC*, 2007].

[4] Aside from precipitation change, air temperature change also affects runoff. Consequently, when scientists evaluated the effect of global warming on the hydrological cycle, they also noticed the drawback of equation (2). To integrate the effect of changing air temperature, *Fu et al.* [2007] proposed the two-parameter climate elasticity:

$$dR/R = \varepsilon_a dP/P + \varepsilon_b dT/T, \quad (3)$$

where ε_a and ε_b are the precipitation elasticity and air temperature elasticity, respectively. Based on this equation, *Fu et al.* [2009] projected the decrease in runoff from the multigeneral circulation model (GCM) outputs from the IPCC Fourth Assessment Report (AR4) and documented potentially serious changes in water resource management in the North China Plain. However, other climatic variables, such as net radiation (R_n) and wind speed at a height of 2 m above ground (U_2), may also influence the hydrologic cycle. To evaluate their effects, we propose a new equation defined as follows:

$$dR/R = \varepsilon_a dP/P + \varepsilon_b dT/T + \varepsilon_c dR_n/R_n + \varepsilon_d dU_2/U_2, \quad (4)$$

where ε_a, ε_b, ε_c, and ε_d are the climate elasticities. However, we do not know yet how many climatic variables need to be considered when assessing climate change effects on runoff and which the dominant variables in theory are.

[5] To project the hydrologic response to climate change, the key process is the estimation of climate elasticity, which can be conducted in different ways. *Sankarasubramanian et al.* [2001] classified these ways into five categories: calibrating a conceptual deterministic watershed model, analytical derivation, fitting a multivariate regional hydrologic model, empirically estimating the relationship between changes in runoff and changes in climate from historical data, and using multivariate statistical methods. Among these methods, the analytical derivation is clear in theory and does not depend on a large amount of historical climate and runoff data, i.e., analytically deriving climate elasticity of annual runoff based on the Budyko hypothesis and then evaluating the impact of climatic variables on runoff. Consequently, this approach has been applied in many studies [*Arora*, 2002; *Dooge et al.*, 1999; *Zheng et al.*, 2009]. The common formulas for the Budyko hypothesis, which are called Budyko-type formulas, are shown in Table 1. *Schaake* [1990] derived the precipitation elasticity of runoff (equation (1)) according to one Budyko-type formula. *Arora* [2002] derived the sensitivity of runoff to changes in precipitation and potential evaporation

$$\frac{\Delta R}{R} = \left[1 + \frac{\phi F_0'(\phi)}{1 - F_0(\phi)}\right]\frac{\Delta P}{P} - \frac{\phi F_0'(\phi)}{1 - F_0(\phi)}\frac{\Delta E_0}{E_0}$$

($\phi = E_0/P$, $F_0(\phi)$ as a Budyko-type formula and $F_0'(\phi)$ as the derivative with respect to ϕ). In Arora's study, five different formulas, namely the Schreiber equation [*Schreiber*, 1904], the Ol'dekop equation [*Ol'dekop*, 1911], the Budyko equation [*Budyko*, 1958], the Turc-Pike equation [*Pike*, 1964; *Turc*, 1954], and the Zhang et al. equation [*Zhang et al.*, 2001] (with $w = 1$) were taken to apply $F_0(\phi)$, and the derivation on the different formulas led to large differences in the climate elasticity. Similarly, *Zheng et al.* [2009] estimated the climate elasticity of runoff for the headwaters of the Yellow River Basin. Following Schaake's idea, *Sankarasubramanian et al.* [2001] drew a contour map of precipitation elasticity of runoff for the continental United States based on the Turc-Pike equation [*Pike*, 1964; *Turc*, 1954]. Two points require more attention: (1) the effects of catchment characteristics on the climate elasticity, and (2) evaluating and separating the effects of other climatic variables (e.g., air temperature and radiation) on runoff.

[6] One motivation of this paper is to provide a framework to assess and separate the effects of different climatic variables on runoff. First, we develop a derivation of climate elasticity of runoff to precipitation and potential evaporation based on the Budyko hypothesis, particularly one that includes the effects of catchment characteristics. Second, we express the change in potential evaporation as a function of changes in net radiation, air temperature, wind speed, and relative humidity, and then further express the runoff change as a function of changes in precipitation, radiation, air temperature, wind speed, and relative humidity to separate the contributions from the changes in climatic variables.

2. Derivation of the Climate Elasticity of Annual Runoff

2.1. Response of Annual Runoff to Climate Change

[7] In a catchment over a long-term time scale, evaporation can be expressed as a function of precipitation and potential evaporation [*Budyko*, 1974]. This is called the Budyko hypothesis. *Yang et al.* [2008] drew an analytical derivation of the Budyko hypothesis:

$$E = \frac{E_0 P}{\left(P^n + E_0^n\right)^{1/n}}, \quad (5)$$

where the parameter n represents the effect of catchment characteristics. Denoting equation (5) as $E = f(E_0, P, n)$, we can express the total differential as

$$dE = \frac{\partial f}{\partial P}dP + \frac{\partial f}{\partial E_0}dE_0 + \frac{\partial f}{\partial n}dn. \quad (6)$$

When evaluating the trend in annual evaporation or runoff for the long term, the water balance equation can be simplified as $P = E + R$ for a catchment. This leads to the differential form $dP = dE + dR$. Its substitution into equation (6) leads to

$$dR = \left(1 - \frac{\partial f}{\partial P}\right)dP - \frac{\partial f}{\partial E_0}dE_0 - \frac{\partial f}{\partial n}dn. \quad (7)$$

[8] Equation (7) describes the response of runoff to climate change as well as to the changes in catchment characteristics.

Table 1. Different Formulas for the Budyko Hypothesis

Formula	Parameter	Reference
$E = P[1 - \exp(-E_0/P)]$	Non	*Schreiber* [1904]
$E = E_0 \tanh(P/E_0)$	Non	*Ol'dekop* [1911]
$E = P/[1 + (P/E_0)^2]^{0.5}$	Non	*Pike* [1964]; *Turc* [1954]
$E = \{P[1 - \exp(-E_0/P)]\, E_0 \tanh(P/E_0)\}^{0.5}$	Non	*Budyko* [1958]
$E = P + E_0 - [P^{\varpi} + E_0{}^{\varpi}]^{1/\varpi}$	ϖ	*Fu* [1981]
$E = P/[1 + (P/E_0)^n]^{1/n}$	n	*Choudhury* [1999]; *Yang et al.* [2008]
$E = P[1 + w(E_0/P)]/[1 + w(E_0/P) + P/E_0]$	w	*Zhang et al.*, [2001]

2.2. Climate Elasticity of Annual Runoff

[9] In equation (7) $dn = 0$ when no consideration is given to the interannual changes in catchment characteristics, i.e.,

$$dR = \left(1 - \frac{\partial f}{\partial P}\right) dP - \frac{\partial f}{\partial E_0} dE_0.$$

We divide this equation using $R = P - E$, and obtain the following:

$$\frac{dR}{R} = \left(1 - \frac{\partial f}{\partial P}\right) \frac{P}{P-E} \frac{dP}{P} - \frac{\partial f}{\partial E_0} \frac{E_0}{P-E} \frac{dE_0}{E_0},$$

which can be denoted as

$$\frac{dR}{R} = \varepsilon_1 \frac{dP}{P} + \varepsilon_2 \frac{dE_0}{E_0}, \tag{8}$$

where the climate elasticity of runoff

$$\varepsilon_1 = \frac{(1 - \partial f/\partial P)P}{P-E}, \quad \varepsilon_2 = -\frac{\partial f/\partial E_0 E_0}{P-E}.$$

Potential evaporation E_0 (mm d^{-1}) can be calculated using the Penman equation [*Penman*, 1948]:

$$\begin{aligned} E_0 = {} & \frac{\Delta}{\Delta + \gamma}(R_n - G)/\lambda \\ & + \frac{\gamma}{\Delta + \gamma} 6.43(1 + 0.536U_2)(1 - RH)e_s/\lambda, \end{aligned} \tag{9}$$

where Δ is the slope of the saturated vapor pressure versus air temperature curve (kPa °C^{-1}), γ is a psychometric constant (kPa °C^{-1}), λ is the latent heat of vaporization of water (MJ kg^{-1}), R_n and G are the net radiation and soil heat flux (MJ m^{-2} d^{-1}), respectively, e_s is the saturated vapor pressure (kPa), RH is the relative humidity (%), and U_2 is the wind speed at a height of 2 m (m s^{-1}).

[10] Modifying the Penman equation [*Penman*, 1948], *Linacre* [1994] devised the PenPan model for estimating pan evaporation (E_p) based on climate data:

$$E_p = \frac{\Delta}{\Delta + 2.4\gamma} R_n/\lambda + \frac{\gamma}{\Delta + 2.4\gamma} f_q(U_2)(1 - RH)e_s/\lambda,$$

where f_q (U_2) is the vapor transfer function. Based on the PenPan model, *Roderick et al.* [2007] developed a differential model to separate the contributions of climatic variable change from change in pan evaporation:

$$dE_p \approx \frac{\partial E_p}{\partial R_n} dR_n + \frac{\partial E_p}{\partial U_2} dU_2 + \frac{\partial E_p}{\partial D} dD + \frac{\partial E_p}{\partial T} dT.$$

Similarly, the contributions of climatic variables to the change in potential evaporation can be estimated:

$$dE_0 \approx \frac{\partial E_0}{\partial R_n} dR_n + \frac{\partial E_0}{\partial T} dT + \frac{\partial E_0}{\partial U_2} dU_2 + \frac{\partial E_0}{\partial RH} dRH. \tag{10}$$

Furthermore,

$$\begin{aligned} \frac{dE_0}{E_0} & \approx \left(\frac{R_n}{E_0}\frac{\partial E_0}{\partial R_n}\right)\frac{dR_n}{R_n} + \left(\frac{1}{E_0}\frac{\partial E_0}{\partial T}\right) dT \\ & \quad + \left(\frac{U_2}{E_0}\frac{\partial E_0}{\partial U_2}\right)\frac{dU_2}{U_2} + \left(\frac{RH}{E_0}\frac{\partial E_0}{\partial RH}\right)\frac{dRH}{RH} \\ & = \varepsilon_3 \frac{dR_n}{R_n} + \varepsilon_4 dT + \varepsilon_5 \frac{dU_2}{U_2} + \varepsilon_6 \frac{dRH}{RH}, \end{aligned} \tag{11}$$

where ε_3, ε_4, ε_5, and ε_6 are the elasticity of potential evaporation with respect to changes in R_n, T, U_2, and RH, respectively.

[11] Combining equations (8) and (11), we obtain the following:

$$\begin{aligned} \frac{dR}{R} & = \varepsilon_1 \frac{dP}{P} + \varepsilon_2\varepsilon_3 \frac{dR_n}{R_n} + \varepsilon_2\varepsilon_4 dT + \varepsilon_2\varepsilon_5 \frac{dU_2}{U_2} + \varepsilon_2\varepsilon_6 \frac{dRH}{RH} \\ & = P^* + R_n^* + T^* + U_2^* + RH^*, \end{aligned} \tag{12}$$

where P^*, R_n^*, T^*, U_2^*, and RH^* represent the changes due to changing P, R_n, T, U_2, and RH, respectively. The climate elasticity indices $\varepsilon_P = \varepsilon_1$, $\varepsilon_{\mathrm{Rn}} = \varepsilon_2\varepsilon_3$, $\varepsilon_T = \varepsilon_2\varepsilon_4$, $\varepsilon_U = \varepsilon_2\varepsilon_5$, and $\varepsilon_{\mathrm{RH}} = \varepsilon_2\varepsilon_6$ in equation (12) show the relative contributions of the corresponding climatic variables to runoff change.

[12] Changing air temperature can alter the atmospheric state, which leads to changing potential evaporation, affecting runoff. Changing air temperature also affects atmospheric movement, which results in changing precipitation, as global warming may cause an overall increase in continental precipitation due to greater evaporation from the oceans [*Gardner*, 2009]. In this study we focus on the direct effect of air temperature on runoff. We digress from the indirect effect of air temperature, i.e., the changing precipitation caused by increasing air temperature, which can be assessed by evaluating the effect of air temperature on precipitation. For example, *Chiew et al.* [2009] assessed the indirect effect of air temperature on runoff based on the mean annual rainfall projection range of −10% to +3% changes per degree global warming from the GCMs.

2.3. Estimation of Climate Elasticity

[13] In many previous studies, climate elasticity was estimated based on mean annual climatic variables [*Arora*, 2002; *Dooge et al.*, 1999; *Zheng et al.*, 2009]. Therefore, equation (12) can be transformed into

$$\begin{aligned} \frac{dR}{\overline{R}} & = \varepsilon_1 \frac{dP}{\overline{P}} + \varepsilon_2\varepsilon_3 \frac{dR_n}{\overline{R}_n} + \varepsilon_2\varepsilon_4 dT + \varepsilon_2\varepsilon_5 \frac{dU_2}{\overline{U}_2} + \varepsilon_2\varepsilon_6 \frac{dRH}{\overline{RH}} \\ & = P^* + R_n^* + T^* + U_2^* + RH^*, \end{aligned} \tag{13}$$

where $\overline{R}$, $\overline{P}$, $\overline{R}_n$, $\overline{T}$, $\overline{U}_2$, and $\overline{RH}$ are the mean annual runoff, precipitation, net radiation, air temperature, wind speed, and relative humidity, respectively. The climate elasticity can be expressed as follows:

$$\varepsilon_1 = \frac{\overline{P}}{\overline{P} - \overline{E}}\left(1 - \left.\frac{\partial f}{\partial P}\right|_{P=\overline{P}, E_0=\overline{E}_0}\right) \text{ and}$$

$$\varepsilon_2 = -\frac{E_0}{P - E}\left(\left.\frac{\partial f}{\partial E_0}\right|_{P=\overline{P}, E_0=\overline{E}_0}\right),$$

where f represents equation (5). Similarly,

$$\varepsilon_3 = \frac{\overline{R}_n}{\overline{E}_0}\frac{\partial E_0}{\partial R_n}\bigg|_{X=\overline{X}}, \quad \varepsilon_4 = \frac{1}{\overline{E}_0}\frac{\partial E_0}{\partial T}\bigg|_{X=\overline{X}},$$

$$\varepsilon_5 = \frac{\overline{U}_2}{\overline{E}_0}\frac{\partial E_0}{\partial U_2}\bigg|_{X=\overline{X}}, \text{ and } \varepsilon_6 = \frac{\overline{RH}}{\overline{E}_0}\frac{\partial E_0}{\partial RH}\bigg|_{X=\overline{X}},$$

where $\overline{(\ )}$ represents the mean annual values of the climatic variables, and $X = \overline{X}$ denotes $R_n = \overline{R}_n, T = \overline{T}, U_2 = \overline{U}_2, RH = \overline{RH}$.

3. Case Study

3.1. Study Region and Data

[14] The Futuo River Basin is located west of the Hai River Basin, Northern China, with the Nanzhuang Hydrologic Station (113°14′E, 38°28′N) as the outlet of the catchment (Figure 1). The catchment size, extracted using a digital elevation model of 1 km resolution, has a drainage area of 12,000 km^2, with relatively few human alterations (e.g., dams and irrigation) to the water balance. Its mean annual potential evaporation (estimated by equation (9)) is 1313 mm a^{-1}, and its mean annual precipitation is 520 mm a^{-1}. The monthly discharge data for this catchment were collected from 1961 to 2000. Daily meteorological data collected in 12 stations from 1961 to 2000 included the mean, maximum, and minimum air temperatures; sunshine duration; wind speed; relative humidity; and precipitation. Daily solar radiation data at four weather stations near this catchment were also collected for this study.

[15] The procedure for calculating the catchment average climatic variables are as follows: (1) a 10 km grid data set covering the study areas was interpolated from the weather station data; (2) potential evaporation was estimated in each grid using equation (9); and (3) the catchment average values were calculated. Air temperature was interpolated using an inverse-distance weighted technique that considers the effect of elevation. Other variables were interpolated using an inverse-distance weighted technique. In the estimation of net radiation, the solar radiation was calculated by the Angstrom Equation [*Allen et al.*, 1998] involving the sunshine duration, where the parameters (a_s and b_s) were calibrated using the observed data for each month at the four stations. The values of a_s and b_s for each grid area were obtained from the nearest station. The first-order estimation of the net long-wave radiation was derived from the relative sunshine duration, surface minimum and maximum air temperature, and vapor pressure without considering the clouds, as per the method recommended by the Food and Agriculture Organization (FAO) of the United Nations [*Allen et al.*, 1998].

3.2. Trend in Climatic and Hydrologic Variables

[16] In section 3.1 the catchment average values of the climatic and hydrologic variables were calculated. We also calculated the mean annual values for the whole catchment and examined the trends of the annual climatic variable series using linear regression. The significance of these trends was analyzed by the Student's t test. The results are shown in Figure 2. The change rate is defined as the ratio of the trend to the mean annual value (Table 2).

[17] As shown in Table 2, the mean annual precipitation $\overline{P}$ and runoff $\overline{R}$ are 520 and 61 mm a^{-1}, respectively, in the period of 1961–2000. Moreover, the mean annual evaporation was $\overline{E}$ from $\overline{E} = \overline{P} - \overline{R} = 459$ mm a^{-1}. After determining $\overline{E}$, $\overline{E_0}$, and $\overline{P}$, parameter n was estimated to be 1.6 according to equation (5).

[18] Figure 2 shows a significant ($p = 0.1$) trend in P, R_n, T, wind speed U_2, RH, and R. U_2 had a fluctuation increase in the period of 1961–1980 and a decrease since 1980. Table 2 shows the following: (1) R_n and U_2 had significant

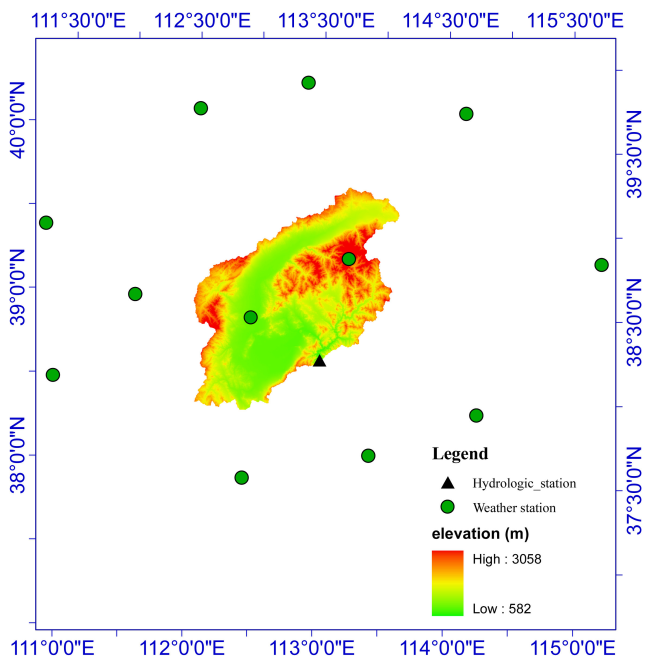

Figure 1. Futuo River basin and the hydrologic and weather stations.

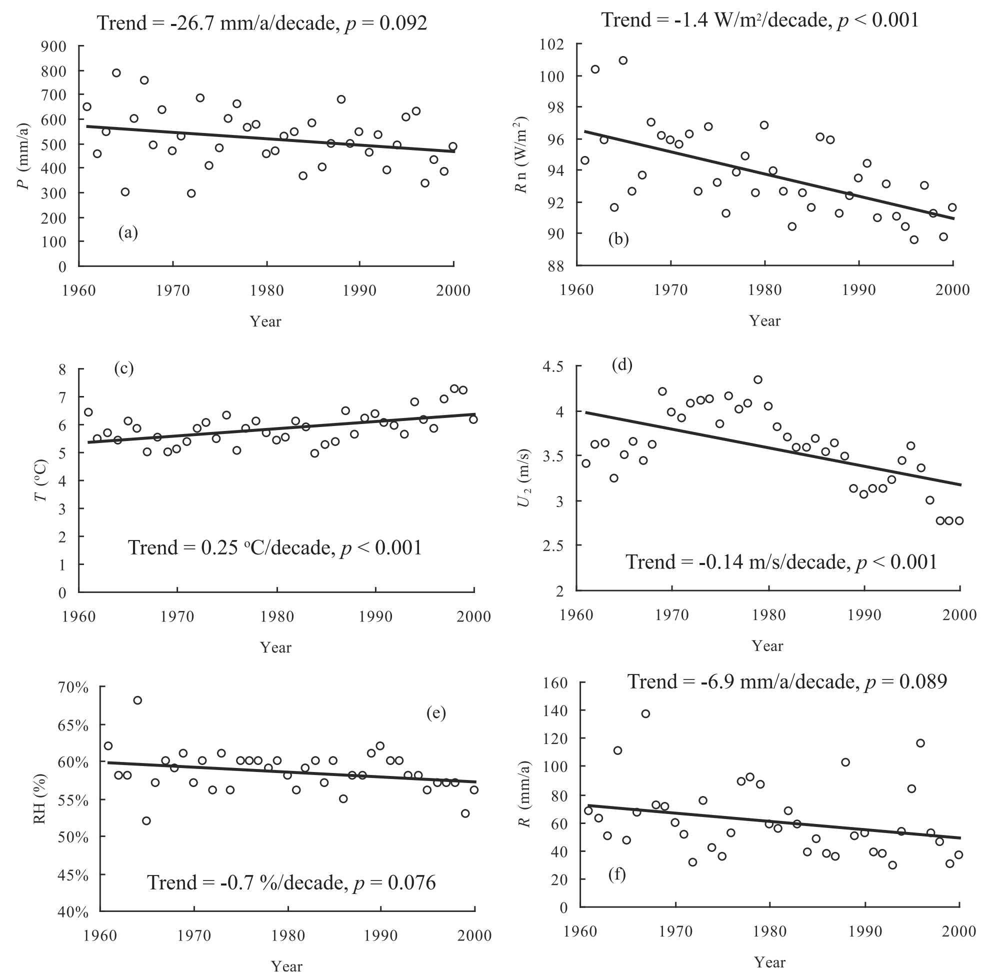

Figure 2. Changes in climatic variables and runoff in the Futuo River basin: (a) annual precipitation, (b) net radiation, (c) air temperature, (d) wind speed at 2 m above ground, (e) relative humidity, and (f) runoff.

reductions ($p < 0.001$); (2) P, RH, and R decreased at a significant level of 0.10; (3) along with P decreasing to -27 mm a^{-1} decade^{-1} (-5% decade^{-1}), R declined to -6 mm a^{-1} decade^{-1} (-10% decade^{-1}); (4) this catchment had been warming at 0.25°C decade^{-1}; (5) R_n had a downward trend of -1.4 W m^{-2} decade^{-1} (approximately -1.5% decade^{-1}); and (6) U_2 had been declining at -0.14 m s^{-1} decade^{-1} (approximately -6% decade^{-1}).

3.3. Climate Elasticity of Runoff

[19] Following section 2.3, we can estimate the climate elasticity according to the mean annual climatic variables, namely, $\varepsilon_1 = 2.36$, $\varepsilon_2 = -1.36$, $\varepsilon_3 = 0.58$, $\varepsilon_4 = 0.035$, $\varepsilon_5 = 0.24$, $\varepsilon_6 = -0.61$. The change in runoff can be evaluated as follows:

$$\frac{dR}{\overline{R}} = 2.4\frac{dP}{\overline{P}} - 0.79\frac{dR_n}{\overline{R_n}} - 0.048dT - 0.33\frac{dU_2}{\overline{U_2}} + 0.83\frac{dRH}{\overline{RH}}. \quad (14)$$

Equation (14) indicates that a 1% P increase will result in 2.4% runoff increase; a 1% increase in R_n and U_2 will lead to 0.79% and 0.33% decrease in runoff, respectively; a 1°C T increase will cause a 4.8% runoff decrease; and a 1% increase in RH will induce 0.83% increase in runoff. The

Table 2. Climatic and Hydrologic Variables in the Futuo River Basin

	Mean Annual	Trend	Significance (p)	Change Rate (% decade^{-1})
E_0	1313 mmol a^{-1}	-24.2 mmol a^{-1} decade^{-1}	0.02	-1.8
P	520 mmol a^{-1}	-26.7 mmol a^{-1} decade^{-1}	0.092	-5.1
R_n	94 W m^{-2}	-1.4 W m^{-2} decade^{-1}	<0.001	-1.5
R_{ns}	139 W m^{-2}	-2.4 W m^{-2} decade^{-1}	<0.001	-1.7
R_{nl}	46 W m^{-2}	-1.0 W m^{-2} decade^{-1}	<0.001	-2.2
T	5.9°C	0.25°C decade $^{-1}$	<0.001	
U_2	2.5 m s^{-1}	-0.14 m s^{-1} decade^{-1}	<0.001	-5.7
RH	59%	-0.7% decade^{-1}	0.076	-1.1
R	60.7 mmol a^{-1}	-5.9 mmol a^{-1} decade^{-1}	0.089	-9.7

value of ε_P is 3–10 times larger than that of the other climatic variable elasticities in this catchment, indicating that runoff is more sensitive to precipitation than to other climatic variables.

[20] Substitution of the change rate of climatic variables into equation (14) leads to $P^* = -12.0\%$ decade^{-1}, $R_n^* =$ 1.2% decade^{-1}, $T^* = -1.2\%$ decade^{-1}, $U_2^* = 1.9\%$ decade^{-1}, and $RH^* = -0.9\%$ decade^{-1}. The runoff change $dR/R = -11\%$ decade^{-1} was calculated. The results show an 11% decade^{-1} decrease in runoff, which is close to the observed change of 10%. The results also indicate that precipitation decrease is the main cause of declining runoff in this catchment, about -12% decade^{-1}. The weakening wind speed had a relatively greater effect on runoff, about 2% decade^{-1}. Moreover, regional warming led to a 1.2% decade^{-1} decline in runoff, which compensated for the positive effect of regional dimming (1.2% decade^{-1}). Wind speed had an equivalent effect to that of air temperature on runoff because of the significant decline in wind speed in the past several decades, e.g., a 28% decrease in the annual mean wind speed over China in the period of 1969–2000 [*Xu et al.*, 2006]. This means that the elasticity of runoff with respect to wind speed needs to be evaluated aside from that to precipitation and air temperature.

3.4. Comparison With Statistics Method

[21] In many previous studies [e.g., *Chiew*, 2006; *Niemann and Eltahir*, 2005; *Novotny and Stefan*, 2007; *Sankarasubramanian and Vogel*, 2003], the climate elasticity was estimated by median descriptive statistics [*Sankarasubramanian et al.*, 2001]:

$$\varepsilon = \text{median}\left[\frac{(R_i - \overline{R})/\overline{R}}{(X_i - \overline{X})/\overline{X}}\right], \tag{15}$$

where X denotes the climatic variables (e.g., P, R_n, and T), and $\overline{R}$ and $\overline{X}$ denote the mean annual runoff and any climatic variable, respectively. The value of

$$\left[\frac{(R_i - \overline{R})/\overline{R}}{(X_i - \overline{X})/\overline{X}}\right]$$

is calculated for each pair of R_i and X_i, and the median of these values is the nonparametric estimator of climate elasticity of runoff ε. Recently, *Zheng et al.* [2009] suggested ε as the linear regression coefficient between $\Delta X_i/\overline{X}$ and $\Delta R_i/\overline{R}$. Elasticity can be estimated using the following least squares estimator:

$$\varepsilon = \frac{\overline{X}}{\overline{R}} \frac{\sum (X_i - \overline{X})(R_i - \overline{R})}{\sum (X_i - \overline{X})^2}. \tag{16}$$

Following equation (15), climate elasticity can be estimated as

$$\varepsilon_P = \text{median}\left[\frac{(R_i - \overline{R})/\overline{R}}{(P_i - \overline{P})/\overline{P}}\right], \quad \varepsilon_{\text{Rn}} = \text{median}\left[\frac{(R_i - \overline{R})/\overline{R}}{(R_{ni} - \overline{R_n})/\overline{R_n}}\right],$$

$$\varepsilon_T = \text{median}\left[\frac{(R_i - \overline{R})/\overline{R}}{(T_i - \overline{T})/\overline{T}}\right],$$

etc., and the runoff change in the Futuo River basin as

$$\frac{dR}{\overline{R}} = 1.30\frac{dP}{\overline{P}} - 0.14\frac{dR_n}{\overline{R_n}} - 0.12dT + 1.21\frac{dU_2}{\overline{U_2}} + 4.61\frac{dRH}{\overline{RH}} = -18\% \text{ decade}^{-1}.$$

Equation (16) estimates

$$\varepsilon_P = \frac{\overline{P}}{\overline{R}} \frac{\sum (P_i - \overline{P})(R_i - \overline{R})}{\sum (P_i - \overline{P})^2}.$$

as well as ε_{Rn}, ε_T, ε_U, and ε_{RH}, and further evaluates the runoff change as

$$\frac{dR}{\overline{R}} = 1.05\frac{dP}{\overline{P}} - 45.9\frac{dR_n}{\overline{R_n}} - 1.09dT + 21.2\frac{dU_2}{\overline{U_2}} + 5.24\frac{dRH}{\overline{RH}} = -64\% \text{ decade}^{-1}.$$

The results show that the runoff change estimated by equation (15) is twice as large as the observed runoff change (approximately -10% decade^{-1}), and the change estimated by equation (16) is up to five times as large. A possible reason for this is the relatively small sample size, which leads to a relatively large error in the climate elasticity [*Zheng et al.*, 2009]. Climate elasticity, given in equation (15), was tested and found to be robust through Monte Carlo experiments for three catchments in the United States [*Sankarasubramanian et al.*, 2001]. Compared with equations (15) and (16), which require large amounts of historical climatic and hydrologic data, the analytical derivation proposed in the present study can estimate climate elasticity based only on the mean annual climate and catchment characteristics (the parameter n).

3.5. Correlation of Net Radiation With Air Temperature

[22] In section 2, R_n and T were considered as two independent variables. R_n is related to T, which includes two parts: net short wave radiation R_{ns} and net long wave radiation R_{nl}:

$$R_n = R_{\text{ns}} - R_{\text{nl}}, \tag{17}$$

R_{nl} can be estimated as follows:

$$R_{\text{nl}} = \varepsilon_s \sigma T^4 (1 - \varepsilon_a), \tag{18}$$

where T is the surface air temperature (K), σ is the Stefan-Boltzman constant (with a value of 5.67×10^{-8} W m^{-2} K^{-4}), ε_s is the surface emissivity (0.98), and ε_a is the clear-sky air emissivity. ε_a can be estimated from the cloudy-sky air emissivity, ε_{ac} [*Lhomme et al.*, 2007]:

$$\varepsilon_a = (-0.34R_s/R_{s0} + 1.37)\varepsilon_{ac}, \tag{19}$$

where R_{s0} is the clear-sky solar radiation, which can be calculated by the method recommended by FAO [*Allen et al.*, 1998]. The value of ε_{ac} was determined using an empirical equation (e.g., the six formulas shown in Table 3).

Table 3. Formulas for Estimating Atmospheric Emissivity Under Clear Skies

Formulas for Clear-Sky Emissivity	Reference
$\varepsilon_{ac} = 0.5893 + 5.351 \times 10^{-2}\sqrt{e_a}$	*Marshunova* [1966]
$\varepsilon_{ac} = 9.294 \times 10^{-6}T^2$	*Swinbank* [1963]
$\varepsilon_{ac} = 1 - 0.26\exp\left[-7.77 \times 10^{-4}(273 - T)^2\right]$	*Idso and Jackson* [1969]
$\varepsilon_{ac} = 1.24\left(\frac{e_a}{T}\right)^{1/7}$	*Brutsaert* [1975]
$\varepsilon_{ac} = 1.08\exp\left(-e_a{}^{T/2016}\right)$	*Satterlund* [1979]
$\varepsilon_{ac} = 0.23 + 0.848\left(\frac{e_a}{T}\right)^{1/7}$	*Konzelmann et al.* [1994]

[23] As a first-order approach, the change in R_{nl} can be expressed as follows:

$$dR_{\mathrm{nl}} = \frac{\Delta R_{\mathrm{nl}}}{\Delta T}dT. \tag{20}$$

For the Futuo River catchment, we calculated the net long wave radiation $R_{\mathrm{nl},1}$ and $R_{\mathrm{nl},2}$ related to $T_1 = 5.4°\mathrm{C}$ and $T_2 = 6.4°\mathrm{C}$ (average air temperature $5.9°\mathrm{C} \mp 0.5°\mathrm{C}$). The value of $\Delta R_{\mathrm{nl}}/\Delta T$ was approximated as

$$\frac{\Delta R_{\mathrm{nl}}}{\Delta T} = \frac{R_{\mathrm{nl},2} - R_{\mathrm{nl},1}}{T_2 - T_1}.$$

Different results were obtained from the different formulas for ε_{ac}, as shown in Table 4. The range covers -0.05 to -01.01 MJ m^{-2} d^{-1} °C^{-1}, with a mean of -0.02 MJ m^{-2} d^{-1} °C^{-1}. When $dR_{\mathrm{nl}} = -0.05dT_a$, the effect on runoff was estimated as $-(\partial E_0/\partial R_{\mathrm{n}})dR_{\mathrm{nl}} = -6.24$ $(-0.05dT) = 0.31dT$; when $dR_{\mathrm{nl}} = 0.01dT$, the effect was -6.24 $(0.54dT) = -0.06dT$. At the same time, the direct effect of T on runoff was $(\partial E_0/\partial T)dT = 35.8dT$. In other words, the relative error was less than 1% if the effect of T on R_n was ignored. Hence, equation (11) is acceptable.

4. Climate Elasticity of Runoff in the Northern Part of China

4.1. Elasticity of Runoff to Precipitation and Potential Evaporation

[24] According to equation (5), we can derive the elasticity of runoff to precipitation ε_P and the elasticity to potential evaporation ε_2 as

$$\varepsilon_P = \left\{1 - 1\Big/[1 + (P/E_0)^n]^{1+1/n}\right\}\Big/\left\{1 - 1\Big/[1 + (P/E_0)^n]^{1/n}\right\} \tag{21}$$

Table 4. Effect of Air Temperature on Net Long-Wave Radiation Estimated by Different Formulas (MJ m^{-2} d^{-1} °C^{-1})

Formulas for Clear-Sky Emissivity	$\Delta R_{\mathrm{nl}}/\Delta T$
Marshunova [1966]	−0.02
Swinbank [1963]	−0.03
Idos and Jackson [1969]	0.01
Brutsaert [1975]	−0.05
Satterlund [1979]	−0.02
Konzelmann et al. [1994]	−0.01
Average	−0.02

and

$$\varepsilon_2 = -\frac{1}{[1 + (E_0/P)^n]^{1+1/n}} \cdot \frac{1}{\frac{1}{E_0/P} - \frac{1}{[1+(E_0/P)^n]^{1/n}}}. \tag{22}$$

The relationship of precipitation elasticity ε_P and potential evaporation elasticity ε_2 with the parameter n and the arid index E_0/P is given in Figure 3. Figure 3 shows that ε_P increases with increasing E_0/P when the parameter n is held constant. In other words, arid regions have larger ε_P and ε_2 than humid regions when they have similar catchment characteristics. Figure 3 also shows that ε_P and ε_2 are sensitive to the parameter n (representing the catchment characteristics) but are much less sensitive to E_0/P, especially in arid and semiarid regions ($E_0/P > 1$). This indicates that catchment characteristics have greater effects on ε_P and ε_2 than climate change (parameterized as E_0/P) has. In particular, ε_P and ε_P are approximately constant when E_0/P is larger than 2. Catchments with a relatively large n has a large ε_P, where the evaporation coefficient E/P is large and the runoff coefficient is small. In other words, precipitation elasticity decreases with the increase in runoff coefficient. This phenomenon was found in 219 catchments across Australia [*Chiew*, 2006].

[25] The parameter n shows a relatively large variability. For example, *Yang et al.* [2007, 2008] found that the parameter n for 108 catchments in the northern part of China, including the Yellow River Basin and the Hai River Basin, was approximately 1.5–3.0. *Choudhury* [1999] found the parameter $n = 2.6$ and $n = 1.8$ in different catchments. However, many previous studies did not pay enough attention to the effect of catchment characteristics on climate elasticity, and thus they attempted to derive climate elasticity based on a single Budyko-type curve. For example, *Sankarasubramanian et al.* [2001] employed the Turc-Pike equation [*Pike*, 1964; *Turc*, 1954] to derive climate elasticity. *Arora* [2002] quantified climate elasticity using different Budyko-type formulas, but he only emphasized the differences among the formulas and did not note the possible causes of the differences. As far as we know, different formulas have been possibly proposed based on data from some basins with different catchment characteristics, implying the effects of catchment characteristics to a certain extent.

[26] The curve ($n \to 0$) describes the relationship of ε_P and ε_2 with the arid index (E_0/P) in catchments with a very low water storage in the subsurface, where ε_P is close to 1 (i.e., 1% precipitation change leading to 1% runoff change) and ε_2 is close to 0. The curve (with large n) describes the relationship of ε_P and ε_2 with E_0/P in the catchments with a very high water storage in the subsurface, such as the plain catchments with a deep quaternary soil layer, where there are large ε_P and ε_2 (i.e., 1% precipitation or potential evaporation change resulting in a volume several times larger than the 1% runoff change).

4.2. Climate Elasticity in the Northern Part of China

[27] In this study, we analyzed the elasticity of runoff to precipitation, net radiation, temperature, wind speed, and relative humidity in 89 catchments in the semiarid and semihumid regions of China located in the northern part,

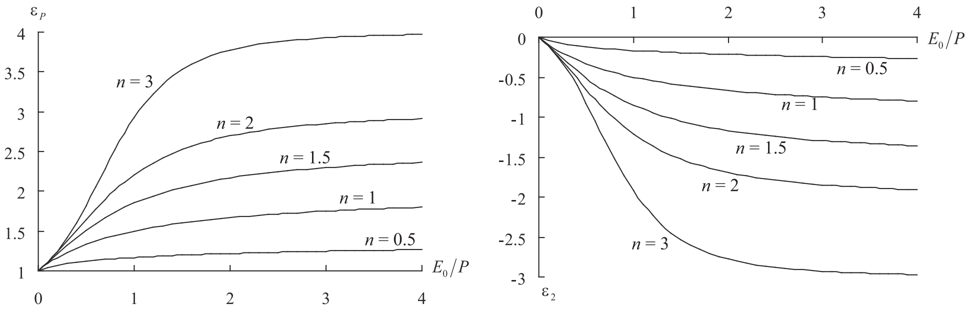

Figure 3. Relationship of the precipitation elasticity ε_P and potential evaporation elasticity ε_2 with the arid index E_0/P and the parameter n.

including the Yellow River Basin and the Hai River Basin. Figure 4 shows the distribution of the 89 study catchments, the basic characteristics of which are listed in Table 5. For more details about the catchments characteristics and data processing see *Yang et al.* [2007]. According to the method proposed in section 2, we calculated the elasticity of runoff to precipitation, net radiation, temperature, wind speed, and relative humidity (Figure 5).

[28] In the 89 catchments, precipitation elasticity ε_P ranged from 1.6 to 3.9 (2.6 on average), indicating that a 1% P change causes 1.6% to 3.9% change in runoff. The high values of $\varepsilon_P > 2.6$ occurred in the middle stream of the Yellow River basin, and the catchments in the Hai River basin and the upstream of the Yellow River basin had relatively small values of $\varepsilon_P < 2.6$. Some previous studies show similar results. For example, *Ma et al.* [2010] estimated $\varepsilon_P = 2.4$ in the Miyun catchment of the Hai River basin using a multiple regression method, and *Zheng et al.* [2009] calculated $\varepsilon_P = 2.1$ in the headwater catchments of the Yellow River basin. However, *Rose* [2009] detected the rainfall-runoff trends in 10 subregions of a 482,000 km^2 in southeastern United States in 1938–2005. The results of his study showed that a 1% change in precipitation results in a 1.2%–2.3% (1.8% on average) change in runoff. Apparently, ε_P for the 10 subregions is statistically less than that for the 89 catchments. The possible reason for this is that the former study regions are in humid regions ($\overline{P}$ of approximately 1200 mm/a), and the latter are in semihumid and semiarid regions (with $\overline{P}$ ranging from 100 to 630 mm/a). *Sankarasubramanian et al.* [2001] revealed the phenomenon that larger values of ε_P occur in more arid regions.

[29] In the 89 catchments, a 1°C increase in temperature produced a 2%–11% (5% on average) decrease in runoff. The large values of $\varepsilon_T < -7\%\ ^\circ\mathrm{C}^{-1}$, mainly occurred in the middle stream of the Yellow River basin, and the catchments of the Hai River basin had $0 > \varepsilon_T > -7\%\ ^\circ\mathrm{C}^{-1}$ (Figure 5c). *Ma et al.* [2010] estimated $\varepsilon_T = -4\%\ ^\circ\mathrm{C}^{-1}$ in the Miyun catchment of the Hai River basin using a multiple regression method. The Hanjiang basin, adjacent to the

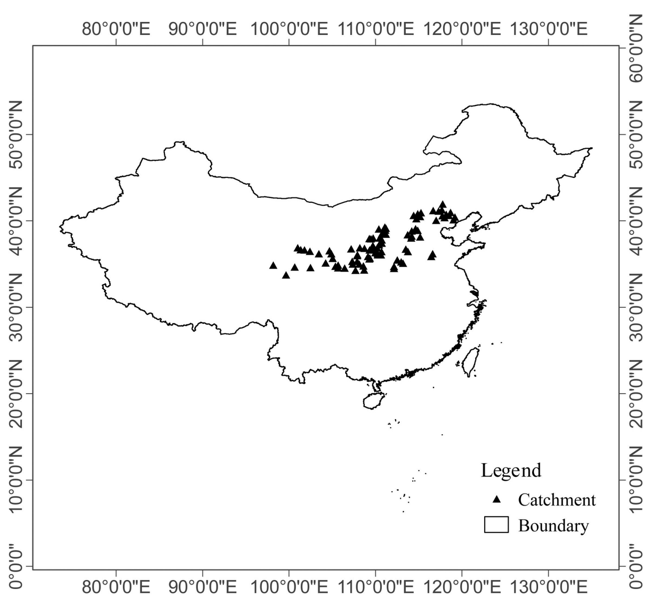

Figure 4. The 89 catchments across the arid regions of Northern China (the triangle placed in the outlet of each catchment).

Table 5. Basic Characteristics of the 89 Catchments in the Northern Part of China

No.	Latitude (°N)	Longitude (°E)	Area (km^2)	$\overline{P}$ (mmol a^{-1})	$\overline{E_p}$ (mmol a^{-1})	n	$\overline{R_n}$ (W m^{-2})	$\overline{T}$ (°C)	$\overline{U_2}$ (m s^{-1})	$\overline{RH}$ (%)
1	117.3	41.12	59.0	484	1187	1.6	100.9	5.91	2.18	55
2	117.74	40.6	127.6	607	1098	1.5	92.2	8.10	1.97	58
3	118	40.37	131.1	622	1060	1.5	86.3	8.43	1.95	59
4	117.76	41.96	42.7	422	1138	1.6	92.3	3.94	2.38	54
5	118.17	40.76	82.1	564	1078	1.8	89.5	7.67	1.72	56
6	117.68	41.3	40.6	452	1149	1.8	98.5	4.89	2.23	55
7	118.49	40.62	117.4	591	1061	1.6	86.1	8.10	1.83	57
8	119.2	40.46	126.6	597	1081	1.5	85.2	8.21	1.98	58
9	118.68	40.98	77.6	551	1050	1.8	83.8	7.24	1.84	55
10	119.04	40.13	143.1	627	1102	1.4	86.2	8.82	2.19	60
11	117.03	40.07	95.6	581	1180	1.6	91.6	9.72	2.17	58
12	116.68	41.2	52.7	443	1234	1.5	98.8	5.30	2.52	55
13	114.42	40.63	28.5	399	1294	1.7	94.9	5.07	3.10	54
14	115.26	40.96	47.6	407	1259	1.5	93.4	3.86	3.06	54
15	114.88	40.82	32.6	396	1295	1.7	92.0	4.51	3.13	53
16	114.73	40.25	16.1	442	1279	2.3	95.3	5.15	3.19	56
17	115.15	40.5	24.4	375	1313	1.7	95.2	4.93	3.14	53
18	114.63	39.08	76.4	495	1323	1.4	96.7	6.05	3.42	58
19	114.88	38.89	59.6	521	1331	1.6	94.1	8.78	3.08	60
20	114.18	38.85	68.1	532	1394	1.5	98.6	7.07	3.67	59
21	113.71	38.39	45.5	518	1310	1.8	93.6	6.30	3.46	58
22	114.13	38.04	60.8	531	1203	1.8	92.0	9.11	2.49	59
23	114.2	38.25	75.4	544	1339	1.5	92.4	10.70	2.92	60
24	115.18	38.16	31.8	548	1365	2.2	93.5	10.75	3.05	61
25	113.5	36.75	59.0	524	1064	1.9	90.7	8.29	1.83	60
26	113.75	36.47	78.4	539	1080	1.7	76.1	10.71	1.87	61
27	98.16	34.89	34.6	346	1137	1.5	116.8	−1.64	2.69	54
28	99.65	33.75	76.2	465	1035	1.5	114.8	−1.86	2.57	60
29	100.64	34.68	183.5	543	1016	1.0	112.1	0.34	2.29	62
30	101	36.91	61.5	365	1109	1.2	107.8	1.56	2.35	54
31	101.36	36.67	87.5	300	1175	0.8	114.1	0.41	2.50	50
32	101.79	36.64	95.4	364	1103	1.0	102.4	2.97	2.23	55
33	102.42	36.48	96.2	359	1098	1.0	100.8	3.88	2.20	56
34	102.48	34.6	197.7	590	972	1.1	109.2	0.85	2.06	64
35	103.44	36.19	25.9	321	1158	1.6	89.8	4.82	2.59	56
36	105.05	35.68	16.1	429	1132	2.4	95.9	6.55	2.70	64
37	104.9	36.2	12.6	395	1152	2.4	91.2	6.61	2.52	62
38	104.69	36.56	11.3	392	1109	2.5	88.2	6.76	2.20	62
39	111.09	39.28	49.9	394	1241	1.4	90.2	6.65	2.41	54
40	111.22	39.17	13.0	441	1182	2.5	90.9	5.40	2.58	56
41	111.03	39.05	64.0	409	1226	1.3	89.6	7.00	2.40	54
42	111.14	38.95	7.9	451	1170	3.0	91.1	5.24	2.62	56
43	111.22	38.47	49.6	450	1147	1.6	94.5	6.03	2.24	56
44	110.4	39.07	55.9	375	1303	1.2	92.7	6.71	2.70	52
45	110.74	38.49	69.0	423	1239	1.3	90.9	8.01	2.37	55
46	110.48	38.03	63.9	428	1216	1.4	91.8	8.28	2.29	55
47	110.74	37.8	48.8	454	1181	1.6	90.7	8.42	2.27	56
48	110.75	37.42	60.7	469	1135	1.6	94.2	7.50	2.15	57
49	109.73	38.03	32.2	349	1267	1.5	92.0	7.80	2.47	53
50	110.42	37.24	35.6	380	1272	1.5	90.3	7.66	2.54	53
51	109.28	37.97	31.5	416	1150	1.8	81.0	7.68	2.19	56
52	109.48	37.93	45.0	425	1205	1.6	84.0	8.30	2.23	55
53	109.7	37.15	43.5	471	1095	1.8	79.5	8.31	2.05	57
54	110.19	36.89	42.6	480	1120	1.9	80.1	9.13	2.06	58
55	110.72	36.47	37.3	502	1090	2.2	86.1	8.93	2.00	60
56	109.81	36.7	37.4	502	1080	2.2	80.0	8.86	1.98	59
57	109.45	36.63	40.9	475	1086	2.0	79.7	8.32	2.02	58
58	109.33	36.63	33.3	496	1080	2.2	80.3	8.56	1.98	59
59	109.99	36.34	19.4	531	1103	3.0	85.1	9.12	1.96	60
60	110.26	36.24	23.7	529	1098	2.8	81.4	9.91	2.01	60
61	110.28	36.08	35.0	554	1139	2.4	87.0	9.35	2.15	61
62	110.65	36.08	43.1	518	1095	2.2	87.1	9.38	2.04	60
63	108.19	36.9	29.3	423	1123	2.0	80.6	7.52	2.15	57
64	108.74	36.84	44.7	458	1081	1.8	79.2	7.63	2.05	58
65	109.34	35.7	27.3	576	1107	2.9	81.8	9.75	2.16	63
66	109.13	35.89	21.2	534	1078	3.0	82.2	8.60	2.03	62
67	109.29	35.61	45.8	579	1099	2.4	84.3	9.34	2.18	64
68	104.22	35.14	38.5	486	965	2.3	84.9	5.77	1.84	66
69	106.43	34.53	19.5	524	1061	3.0	106.4	8.70	1.99	66
70	107.7	34.3	85.1	637	1015	2.2	103.2	10.67	1.65	69

Table 5. (continued)

No.	Latitude (°N)	Longitude (°E)	Area (km^2)	$\overline{P}$ (mmol a^{-1})	$\overline{E_p}$ (mmol a^{-1})	n	$\overline{R_n}$ (W m^{-2})	$\overline{T}$ (°C)	$\overline{U}_2$ (m s^{-1})	$\overline{RH}$ (%)
71	108.7	34.31	75.9	680	1014	2.6	83.6	12.44	1.71	70
72	105.37	34.77	22.1	478	1063	2.5	107.0	7.06	2.32	66
73	105.67	34.9	32.4	471	1106	2.1	101.2	7.06	2.50	65
74	105.69	34.57	43.4	534	1062	2.3	106.3	8.84	1.93	66
75	108.59	34.8	46.4	599	1041	2.6	82.3	9.79	2.17	66
76	107.32	35.32	51.6	512	1071	2.0	94.2	7.85	2.16	65
77	108.14	35.01	38.6	516	1085	2.2	90.0	8.67	2.19	64
78	107.18	36.77	15.7	377	1224	2.0	95.8	7.49	2.43	56
79	107.88	36	21.0	454	1132	2.3	92.1	8.03	2.25	60
80	107.9	36.08	28.9	480	1086	2.3	84.6	8.06	2.08	61
81	107.88	35.33	24.8	540	1088	2.8	86.6	8.88	2.12	63
82	107.39	35.02	39.0	564	1066	2.5	102.6	9.45	1.90	66
83	112.15	34.52	122.5	645	1131	1.6	85.9	12.76	2.19	65
84	112.15	34.72	94.1	605	1149	1.7	85.2	13.08	2.19	64
85	112.52	35.47	77.0	537	1086	1.7	89.2	9.60	1.94	61
86	113.2	35.1	38.0	609	1210	2.5	86.5	14.24	2.36	65
87	112.98	35.25	67.8	580	1081	2.0	82.2	10.72	2.13	64
88	116.45	35.9	81.2	700	1353	2.0	86.2	13.11	3.34	65
89	116.62	36.19	59.9	712	1374	2.3	86.1	12.88	3.45	64
Mean	110.55	37.32	55.9	493	1150	1.9	91.6	7.5	2.34	59
Min.	98.16	33.75	7.9	300	965	0.8	76.1	−1.9	1.65	50
Max.	119.20	41.96	197.7	712	1394	3.0	116.8	14.2	3.67	70

Yellow River basin, had a value of $\varepsilon_T = -4\%$ °C^{-1} [*Chen et al.*, 2007]. They agree with our results. A 1% R_n change produced between −0.3% and −1.9% (−1.0% on average) runoff. Relatively small values of $-0.7 < \varepsilon_{\mathrm{Rn}} < -1.0$ occurred in the catchments in the Hai River basin, and the smallest values occurred upstream of the Yellow River basin. The values of ε_U and $\varepsilon_{\mathrm{RH}}$ ranged from −0.1 to −0.8 (−0.4 on average) and from 0.2 to 1.9 (1.0 on average), respectively.

[30] The relatively small values of elasticities primarily occurred upstream of the Yellow River basin and the Hai River basin, whereas the relatively larger values primarily occurred in the middle stream of the Yellow River basin. *Wang et al.* [2002] analyzed the effects of climate change on runoff in the Yellow River basin using a monthly hydrological model; their results showed smaller elasticities ($\varepsilon_P = 1.2$ and $\varepsilon_T = -4.0\%$ °C^{-1}) in the upstream and larger ones ($\varepsilon_P = 1.9$ and $\varepsilon_T = -5.2\%$ °C^{-1}) in the middle stream, consistent with ours.

[31] In addition, eight catchments, where the runoff data length is more than 35 years and the annual runoff ($p <$ 0.05) has significant trends, were chosen to analyze the attribution of runoff change. Similar to section 3.2, trends in annual climatic variables and runoff series were detected using linear regression. The contributions of climatic variables to runoff change P^*, R_n^*, T^*, U_2^*, RH^* were estimated, the sum of which was the calculated runoff change $dR/\overline{R}|_{\mathrm{cal}}$. The observed runoff change $dR/\overline{R}|_{\mathrm{obs}}$ was detected using linear regression, which was close to $dR/\overline{R}|_{\mathrm{cal}}$ (Table 6). However, the differences between $dR/\overline{R}|_{\mathrm{obs}}$ and $dR/\overline{R}|_{\mathrm{cal}}$ are notable. The possible causes are the following: (1) $dR/\overline{R}|_{\mathrm{cal}}$ was calculated when the impact of land cover change was ignored and (2) some climatic variables have relatively large variabilities but no significant trends. As shown in Table 6, P decrease was primarily responsible for the runoff change in the eight catchments, and its effect was much larger than that of the other variables. In these catchments, the effect of increasing T on runoff was negative, which was fortunately compensated by the decrease in wind speed and net radiation. However, "global brightening" has been apparent since the 1980s, as revealed in many studies [e.g., *Wild*, 2009]. This implies a negative effect on runoff and aggravation of the shortage of water resources.

5. Conclusion

[32] Climate elasticity is widely used to assess the response of runoff to climate change. In this study we analytically derived climate elasticity to assess hydrologic response to climate change by expanding the first-order differential of the mean annual water-energy balance equation [*Choudhury*, 1999; *Yang et al.*, 2008] and the Penman equation [*Penman*, 1948]. Based on the mean annual values of the climatic variables, the climate elasticity of runoff can be estimated to separate the effects of climatic variables (i.e., P, T, R_n, U_2, and RH) on runoff. The effect of catchment characteristics on climate elasticity can be described by adjusting the parameter n. Climate elasticity is sensitive to the parameter n (representing the catchment characteristics).

[33] The Futuo River Basin, located in the Hai River Basin of Northern China, has significant changes in climatic variables, namely, P decreasing at 26.7 mm a^{-1} decade^{-1}, R_n decreasing at −1.4 W m^{-2} decade^{-1}, T increasing at 0.37°C decade^{-1}, U_2 declining at −0.14 m s^{-1} decade^{-1}, and RH decreasing at −0.7% decade^{-1}, which lead to a −10% decade^{-1} runoff change. The 1% increase in P, R_n, U_2, and RH results in a 2.4% increase, 0.8% decrease, 0.3% decrease, and 0.8% increase in runoff, respectively. A 1°C T increase produces a 5% runoff decrease. In this catchment, P decrease is the main cause of the runoff decline; U_2 decline has the second greatest effect.

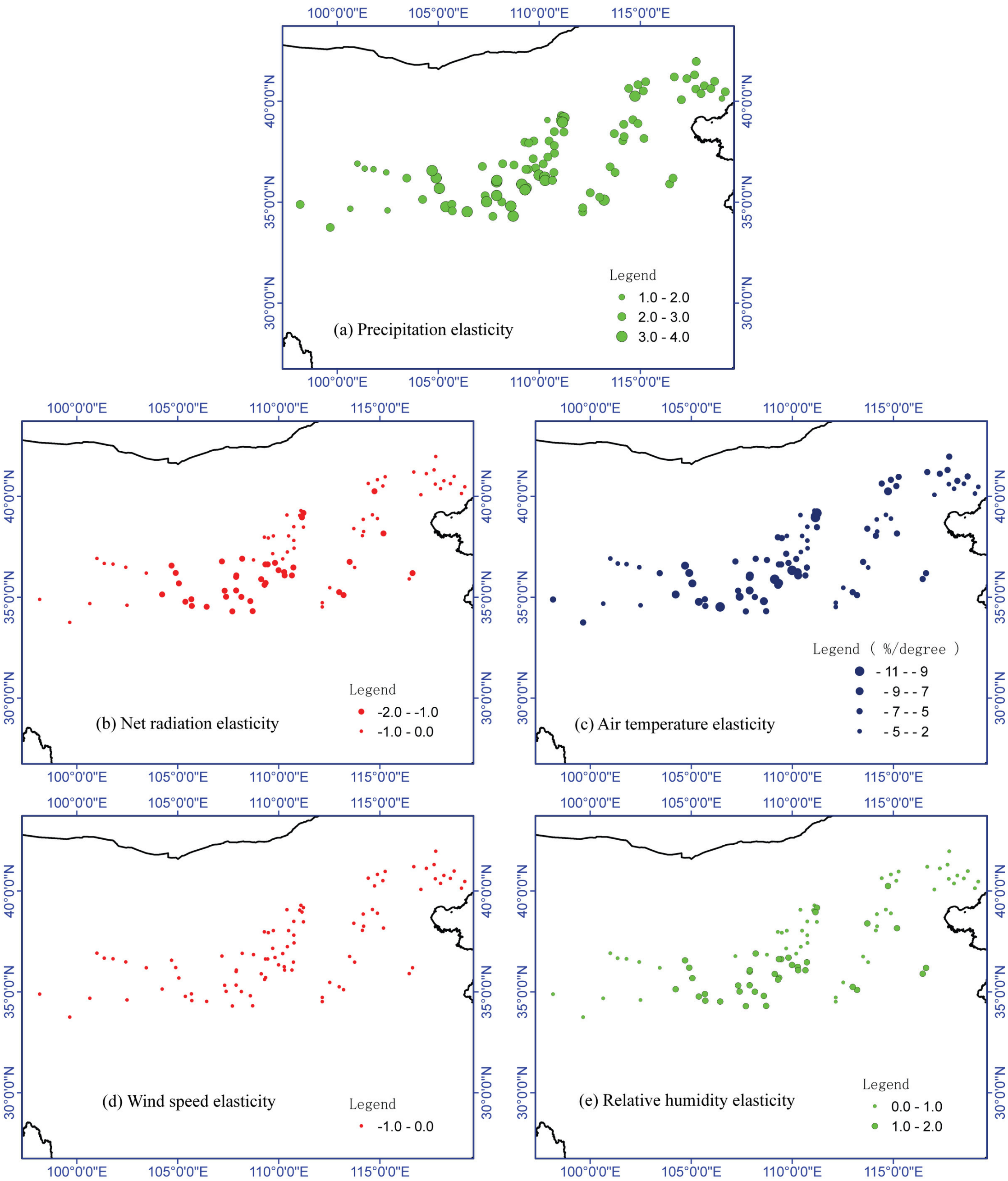

Figure 5. Elasticity of annual runoff to (a) precipitation, (b) net radiation, (c) air temperature, (d) wind speed, and (e) relative humidity in the 89 catchments.

[34] Precipitation elasticity ε_P and potential evaporation elasticity ε_2 are sensitive to catchment characteristics and relatively insensitive to climate (the arid index E_0/P), especially when $E_0/P > 2$. ε_P and ε_2 increase with E_0/P under similar catchment characteristics. By holding the arid index constant, the absolute values of both ε_P and ε_2 increase with the increasing parameter n (e.g., the capacity holding water increasing).

[35] In the 89 catchments across the Hai River and the Yellow River basins of Northern China, a 1% P change leads to a 1.6%–3.9% runoff change, and a 1°C T increase produces a 2%−11% runoff decrease. A 1% change in R_n, U_2, and RH causes −0.3% to −1.9%, −0.1% to −0.8%, and 0.2%–1.9% change in runoff, respectively. Among the 89 catchments, eight catchments were chosen to analyze the attribution of runoff change, where precipitation decrease was primarily responsible for the runoff change, and the effect of increasing T on runoff was negative, which was fortunately compensated by the decrease in U_2 and R_n. However, "global brightening" has been apparent since the 1980s, as revealed in many studies [e.g., *Wild*, 2009]. This implies a negative effect on runoff and aggravation of the shortage of water resources.

Table 6. Attribution of Annual Runoff Change in Eight Catchments[a]

No.	P^*	R_n^*	T^*	U_2^*	RH^*	$\frac{dR}{R}\big\vert_{\text{cal}}$	$\frac{dR}{R}\big\vert_{\text{obs}}$
37	−17.5	0.6	−1.3	0.3	0.0	−18	−27
38	−13.9	0.5	−1.3	0.3	0.1	−14	−12
39	−14.3	0.6	−1.4	0.4	0.0	−15	−11
45	−7.2	0.5	−0.2	1.3	0.0	−6	−7
49	−10.1	0.8	−1.3	0.4	−1.2	−11	−10
70	−12.2	1.7	−0.8	0.6	−0.4	−11	−27
75	−17.9	2.0	−1.4	2.0	−0.9	−16	−8
77	−13.2	1.2	−1.6	2.0	−0.5	−12	−19

[a]In the eight catchments, length of runoff data time series was more than 36 years, and annual runoff with a significant trend a = 0.05. Unit: % decade^{-1}.

[36] **Acknowledgments.** This research was supported by the National Natural Science Foundation of China (50909051 and 51009148) and the public-benefit project of the Ministry of Water Resources P. R. China (200801012). The authors would like to express their appreciation to the editors and four anonymous reviewers, whose comments and suggestions led to significant improvements in the manuscript.

References

Allen, R. G., L. S. Pereira, D. Raes, and M. Smith (1998), *Crop Evapotranspiration: Guidelines for Computing Crop Water Requirements*, Food and Agriculture Organization, Rome.

Arora, V. K. (2002), The use of the aridity index to assess climate change effect on annual runoff, *J. Hydrol.*, *265*(1–4), 164–177.

Brutsaert, W. (1975), On a derivable formula for long-wave radiation from clear skies, *Water Resour. Res.*, *11*(5), 742–744, doi:10.1029/WR011i005p00742.

Budyko, M. I. (1958), *The Heat Balance of the Earth's Surface*, U.S. Department of Commerce, Washington, D. C.

Budyko, M. I. (1974), *Climate and Life*, Academic, New York.

Chen, H., S. L. Guo, C. Y. Xu, and V. P. Singh (2007), Historical temporal trends of hydro-climatic variables and runoff response to climate variability and their relevance in water resource management in the Hanjiang basin, *J. Hydrol.*, *344*(3–4), 171–184.

Chiew, F. H. S. (2006), Estimation of rainfall elasticity of streamflow in Australia, *Hydrolog. Sci. J.*, *51*(4), 613–625.

Chiew, F. H. S., J. Teng, J. Vaze, and D. G. C. Kirono (2009), Influence of global climate model selection on runoff impact assessment, *J. Hydrol.*, *379*(1–2), 172–180.

Choudhury, B. J. (1999), Evaluation of an empirical equation for annual evaporation using field observations and results from a biophysical model, *J. Hydrol.*, *216*(1–2), 99–110.

Dooge, J. C. I. (1992), Sensitivity of runoff to climate change: A Hortonian approach, *Bull. Am. Meteorol. Soc.*, *73*(12), 2013–2024.

Dooge, J. C., M. Bruen, and B. Parmentier (1999), A simple model for estimating the sensitivity of runoff to long-term changes in precipitation without a change in vegetation, *Adv. Water Resour.*, *23*(2), 153–163.

Fu, B. P. (1981), On the calculation of the evaporation from land surface, *Scientia Atmospherica Sinica*, *5*(1), 23–31 (in Chinese).

Fu, G., S. P. Charles, and F. H. S. Chiew (2007), A two-parameter climate elasticity of streamflow index to assess climate change effects on annual streamflow, *Water Resour. Res.*, *43*, W11419, doi:10.1029/2007WR005890.

Fu, G., S. P. Charles, J. Yu, and C. Liu (2009), Decadal climatic variability, trends, and future scenarios for the North China plain, *J. Climate*, *22*(8), 2111–2123.

Gardner, L. R. (2009), Assessing the effect of climate change on mean annual runoff, *J. Hydrol.*, *379*(3–4), 351–359.

Idso, S. B., and R. D. Jackson (1969), Thermal radiation from the atmosphere, *J. Geophys. Res.*, *74*, 5397–5403, doi:10.1029/JC074i023p05397.

IPCC (2007), *Observation: Surface and Atmospheric Climate Change*, edited by K. E. Trenberth and P. D. Jones, Cambridge University Press, Cambridge, UK.

Konzelmann, T., R. Vandewal, W. Greuell, R. Bintanja, E. Henneken, and A. Abeouchi (1994), Parameterization of global and longwave incoming radiation for the Greenland ice-sheet, *Global Planet Change*, *9*(1–2), 143–164.

Lhomme, J. P., J. J. Vacher, and A. Rocheteau (2007), Estimating downward long-wave radiation on the Andean Altiplano, *Agr. Forest Meteorol.*, *145*(3–4), 139–148.

Linacre, E. T. (1994), Estimating United States class—A pan evaporation from few climate data, *Water Int.*, *19*(1), 5–14.

Ma, H. A., D. W. Yang, S. K. Tan, B. Gao, and Q. F. Hu (2010), Impact of climate variability and human activity on streamflow decrease in the Miyun Reservoir catchment, *J. Hydrol.*, *389*(3–4), 317–324.

Marshunova, M. S. (1966), Principal characteristics of the radiation balance of the underlying surface, in *Soviet Data on the Arctic Heat Budget and Its Climate Influence*, edited by J. O. Fletcher et al., Rand Corporation, Santa Monica, CA.

Milly, P. C., and K. A. Dunne (2002), Macroscale water fluxes—2. Water and energy supply control of their interannual variability, *Water Resour. Res.*, *38*(10), 1206, doi:10.1029/2001WR000760.

Niemann, J. D., and E. A. B. Eltahir (2005), Sensitivity of regional hydrology to climate changes, with application to the Illinois River basin, *Water Resour. Res.*, *41*, W07014, doi:10.1029/2004WR003893.

Novotny, E. V., and H. G. Stefan (2007), Stream flow in Minnesota: Indicator of climate change, *J. Hydrol.*, *334*(3–4), 319–333.

Ol'dekop, E. M. (1911), On evaporation from the surface of river basins, *Trans. Meteorol. Obs. Univ. Tartu*, *4*, 200.

Penman, H. L. (1948), Natural evaporation from open water, bare soil and grass, *Proc. R. Soc. London Ser. A.*, *193*(1032), 120–145.

Pike, J. G. (1964), The estimation of annual run-off from meteorological data in a tropical climate, *J. Hydrol.*, *2*(2), 116–123.

Roderick, M. L., L. D. Rotstayn, G. D. Farquhar, and M. T. Hobbins (2007), On the attribution of changing pan evaporation, *Geophys. Res. Lett.*, *34*, L17403, doi:10.1029/2007GL031166.

Rose, S. (2009), Rainfall-runoff trends in the south-eastern USA: 1938–2005, *Hydrol. Processes*, *23*(8), 1105–1118.

Sankarasubramanian, A., and R. M. Vogel (2003), Hydroclimatology of the continental United States, *Geophys. Res. Lett.*, *30*(7), 1363, doi:10.1029/2002GL015937.

Sankarasubramanian, A., R. M. Vogel, and J. F. Limbrunner (2001), Climate elasticity of streamflow in the United States, *Water Resour. Res.*, *37*(6), 1771–1781, doi:10.1029/2000WR900330.

Satterlund, D. R. (1979), Improved equation for estimating long-wave-radiation from the atmosphere, *Water Resour. Res.*, *15*(6), 1649–1650, doi:10.1029/WR015i006p01649.

Schaake, J. C. (1990), From climate to flow, in *Climate Change and U.S. Water Resources*, edited by Waggoner, pp. 177–206, John Wiley, New York.

Schreiber, P. (1904), Ueber die Beziehungen zwischen dem Niederschlag und der Wasserfvhrung der flvsse in Mitteleuropa, *Meteorol. Z.*, *21*, 441–452.

Swinbank, W. C. (1963), Long-wave radiation from clear skies, *Q. J. R. Meteor. Soc.*, *89*(381), 339–348.

Turc, L. (1954), Le bilan d'eau des sols. Relations entre les precipitations, l'evaporation et l'ecoulement, *Ann. Agronomy*, *5*, 491–596.

Wild, M. (2009), Global dimming and brightening: A review, *J. Geophys. Res.*, *114*, D00D16, doi:10.1029/2008JD011470.

Wang, G. Q., Y. Z. Wang, and L. L. Kang, (2002), Analysis on the sensitivity of runoff in Yellow River to climate change, *Q. J. Appl. Meteorol. Sci.*, *13*(1), 117–121 (in Chinese).

Xu, M., C. P. Chang, C. B. Fu, Y. Qi, A. Robock, D. Robinson, and H. M. Zhang (2006), Steady decline of east Asian monsoon winds, 1969–2000: Evidence from direct ground measurements of wind speed, *J. Geophys. Res.*, *111*, D24111, doi:10.1029/2006JD007337.

Yang, D. W., F. B. Sun, Z. Y. Liu, Z. T. Cong, G. H. Ni, and Z. D. Lei (2007), Analyzing spatial and temporal variability of annual water-energy balance in nonhumid regions of China using the Budyko hypothesis, *Water Resour. Res.*, *43*, W04426, doi:10.1029/2006WR005224.

Yang, H. B., D. W. Yang, Z. D. Lei, and F. B. Sun (2008), New analytical derivation of the mean annual water-energy balance equation, *Water Resour. Res.*, *44*, W03410, doi:10.1029/2007WR006135.

Zhang, L., W. R. Dawes, and G. R. Walker (2001), Response of mean annual evapotranspiration to vegetation changes at catchment scale, *Water Resour. Res.*, *37*(3), 701–708, doi:10.1029/2000WR900325.

Zheng, H., L. Zhang, R. Zhu, C. Liu, Y. Sato, and Y. Fukushima (2009), Responses of streamflow to climate and land surface change in the headwaters of the Yellow River Basin, *Water Resour. Res.*, *45*, W00A19, doi:10.1029/2007WR006665.

D. Yang and H. Yang, State Key Laboratory of Hydro-Science and Engineering, Department of Hydraulic Engineering, Tsinghua University, Beijing 100084, China. (yangdw@tsinghua.edu.cn; yanghanbo@tsinghua.edu.cn)